[Geophysical Research Letters]

Supporting Information for

Christine A. Shields[1], Nan Rosenbloom[1], Susan Bates[1], Cecile Hannay[1], Aixue Hu[1], Ashley E. Payne[2], Jonathan J. Rutz[3], John Truesdale[1]

[1]National Center for Atmospheric Research, Boulder, Colorado, 80302

[2]University of Michigan, Ann Arbor, MI 48109

[3]National Oceanic and Atmospheric Administration, Salt Lake City, UT 84138

Contents of this file

Introduction

Supplemental material includes 10 figures and 2 tables and provide further details for parts of this work.

Figure S1 and S2 present AR tracking statistics for CESM1.3 historical model output and MERRA-2 reanalysis using SK2016 detection algorithm, years 1960-2016 and 1991-2005, respectively, as a means of model validation. Climatology for years 1991-2005 are given separately to show that data applied to the heat transport analysis are representative of the longer climatology.

Figures S3–S4 highlight spatial maps for latent and sensible heat terms for AR-days across the climate change projections as seen in Figure 3.

Figures S5-S8 provide reference for Hovmöller Figures 4 and 5 by showing the meridional wind and its variance for the historical and RCP8.5 simulations. Although variability is typically higher

in the cool season, the greatest variance in the meridional wind at all levels is poleward of 60N for both simulation types.

Figures S9-S10 provide a holistic view of the remaining state variables used in meridional heat transport calculations, i.e. air temperature and specific humidity. Both temperature and specific humidity increase under global warming, although there are seasonal and spatial variations in magnitude. The warming and moistening of the background state certainly contribute to the changes in heat transport, however, Figures S9-S10 support the notion that the primary driver of climate change for meridional heat transport is the upper-level meridional wind.

Table S1 summarizes the ARTMIP Tier 1 catalogues used in this analysis; and Table S2 summarizes the CESM1.3 model output data. For CESM1.3 model data, due to data loss, segments of this work do not apply all 3 ensemble members. Table S2 outlines which data was used for which analysis topics.

Figure S1. AR frequency climatology for landfalling storms in CESM1.3 (years 1960-2005, solid bars) compared to MERRA-2 reanalysis (years 1980-2016, dotted bars) using Shields-Kiehl (2016a; 2016b) detection algorithm. Ensemble range is represented by black error bars. Climatologies are shown for the Pacific Northwest (PNW, 41°-52.5°N), California (CA, 32°-41°N), Southern California (SoCal, 32°-35°N), the United Kingdom (UK 49°-60°N), and the Iberian Peninsula (Ib, 35°-49°N). The Shields-Kiehl methodology was designed to detect stronger storms (compared to the mean) appropriate for both historical and global warming scenarios. To see how this algorithm differs from other detection algorithms see ARTMIP results Shields et al. 2018, Rutz et al. (in revision). Climate change AR frequency climatology is consistent with Shields and Kiehl 2016b.

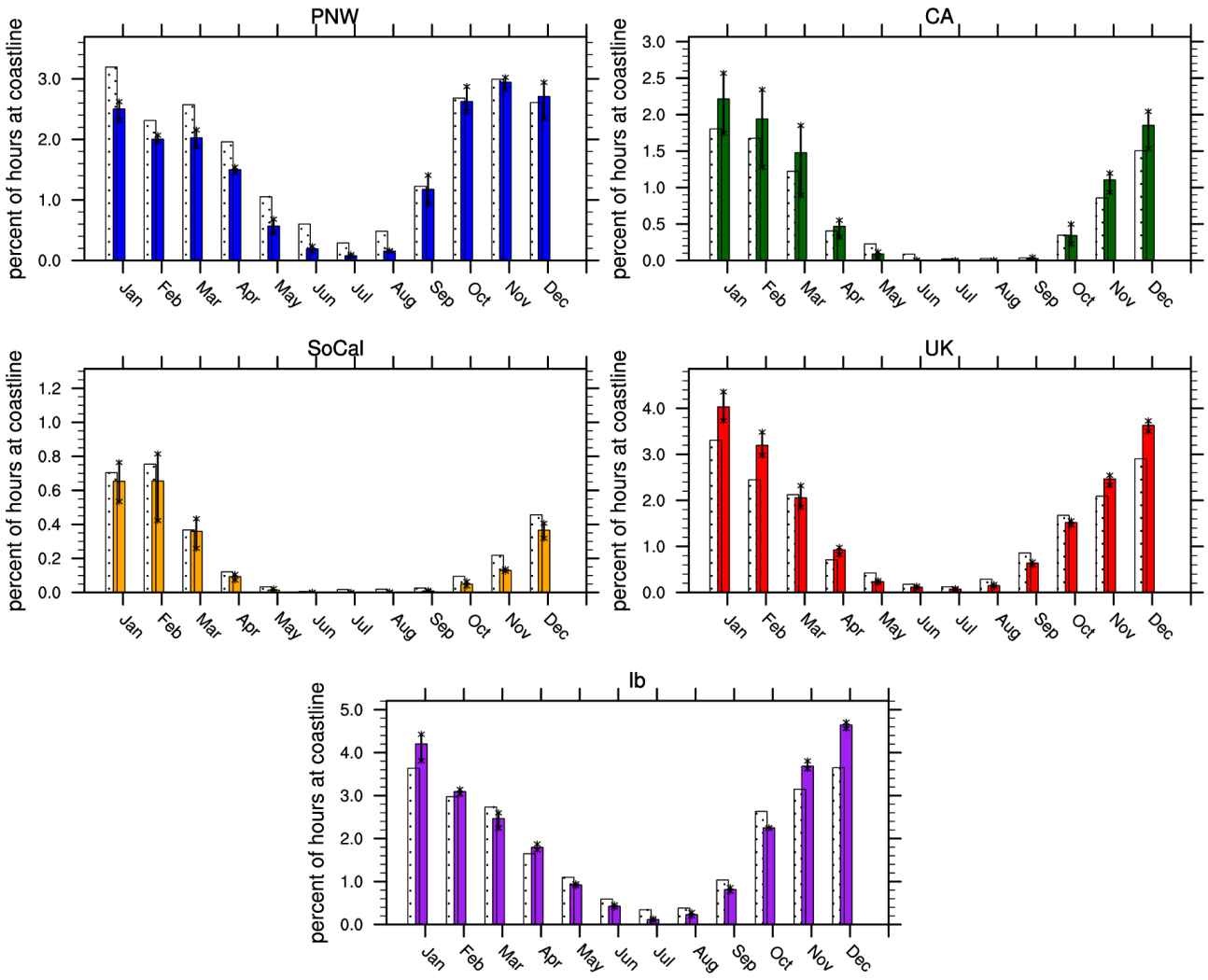

Figure S2. Same as Figure S1, except for years 1991-2005.

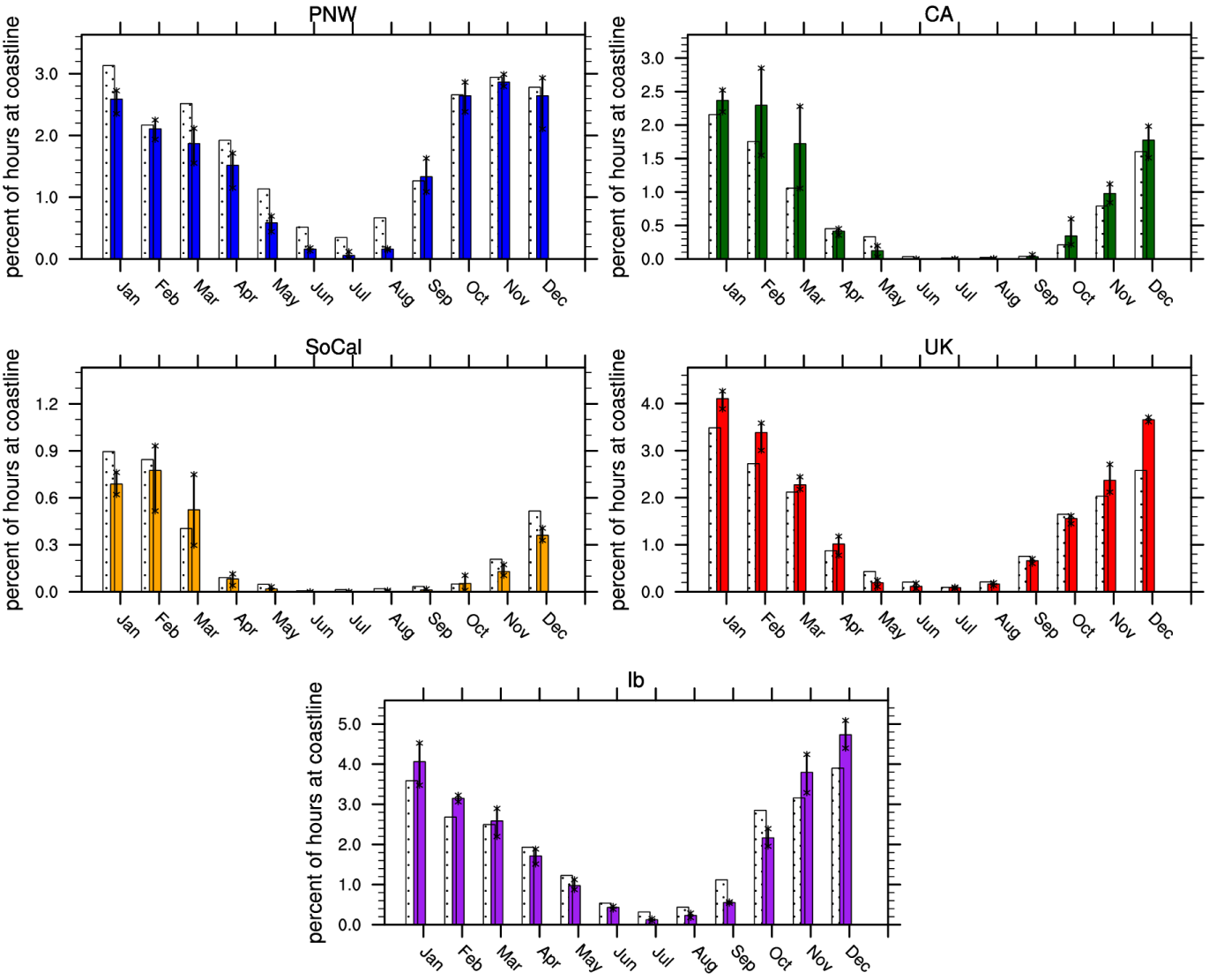

Figure S3. Sensible heat transport term for AR-days over Western North America (left panels), the United Kingdom (middle panels), and the Iberian Peninsula (right panels). The historical period is shown for the upper panels, RCP8.5 for the central panels, and the difference on the bottom panels. Units are in kg ms^{-3} x 10^9.

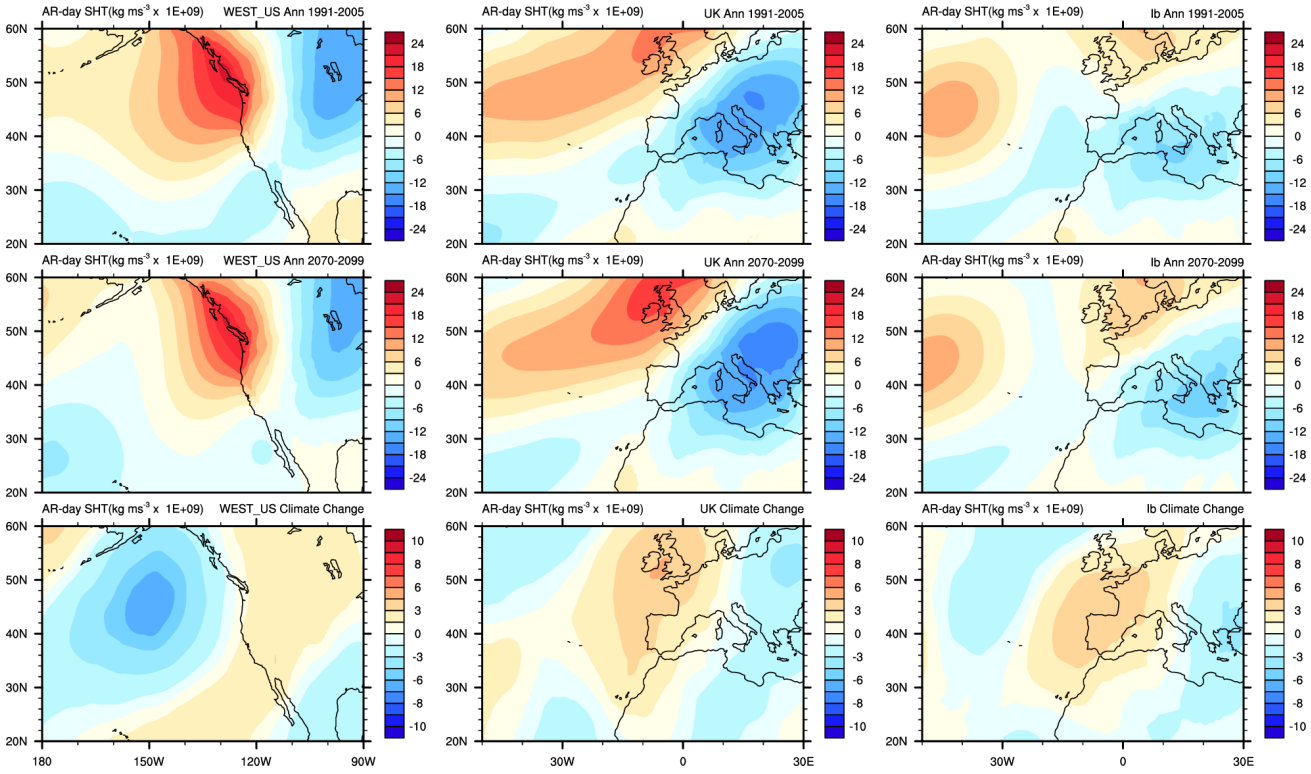

Figure S4. Same as Figure S2 except for latent heat transport term.

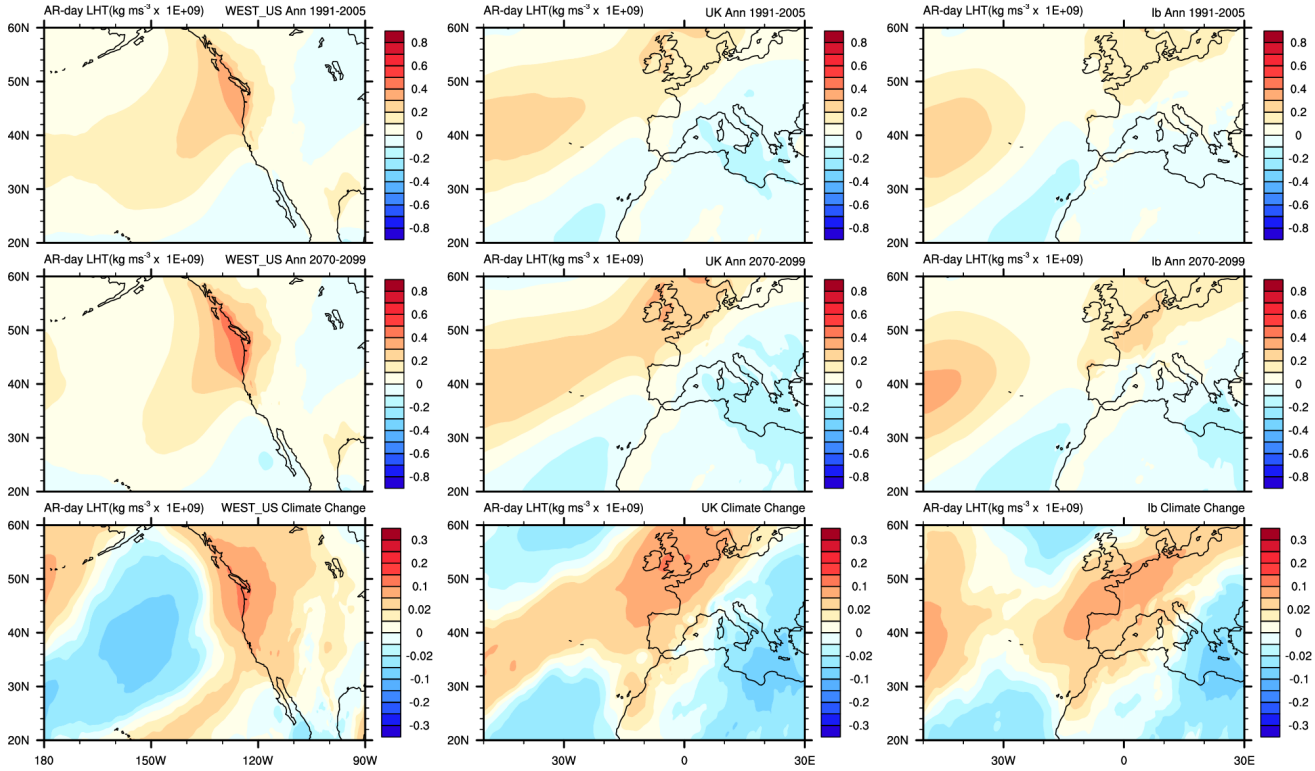

Figure S5. Western North American meridional wind (ms^{-1}, left panels) and its variance (m^2s^{-2}, right panels) for 300 hPa historical (upper panels) and RCP8.5 simulation (lower panels), for broader, "life cycle" domain (180W – 90W). Contour intervals for wind plots range from -15 to + 15 ms^{-1} and variance plots range from -25 to +30 m^2s^{-2}.

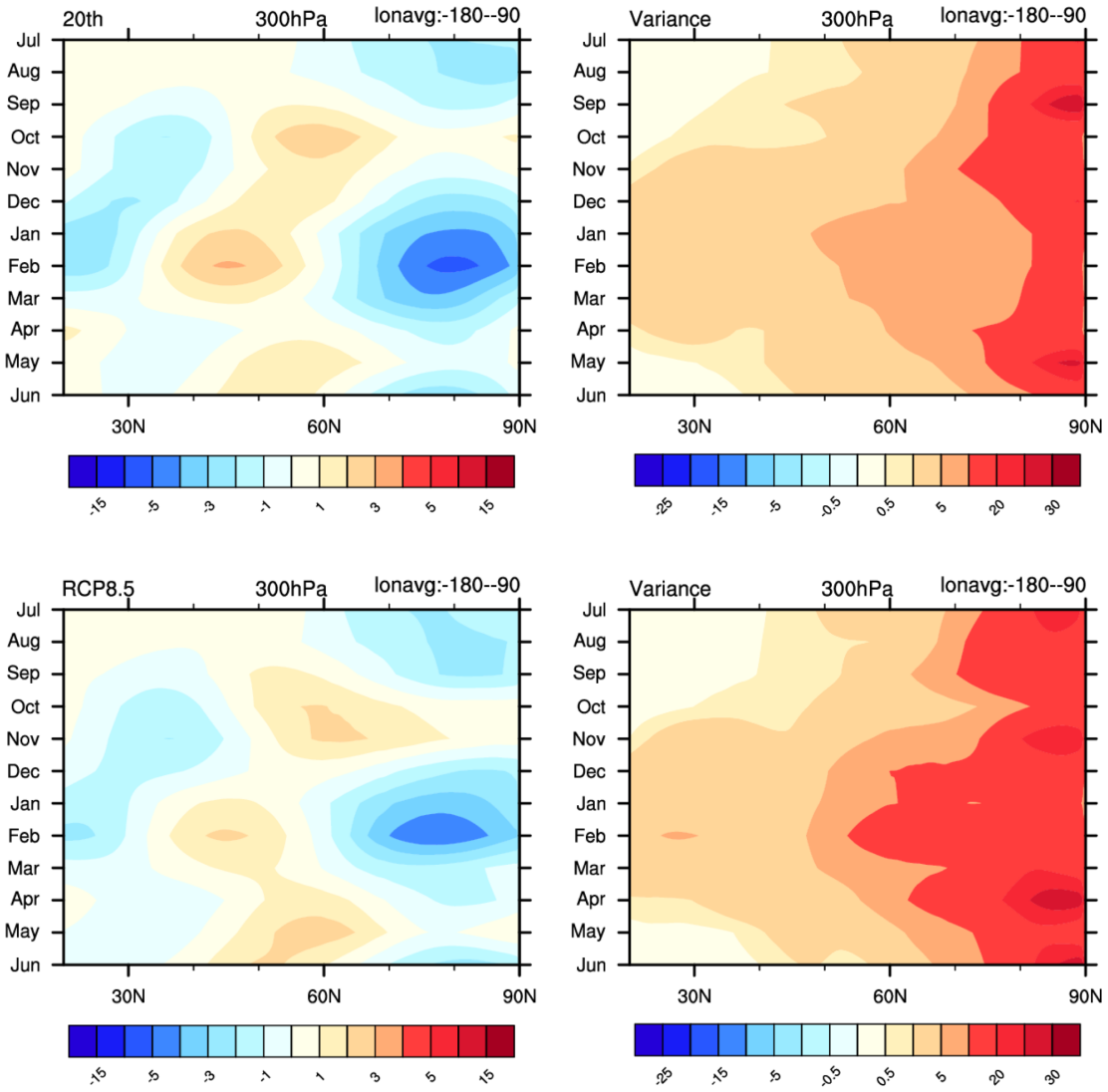

Figure S6. Same as Figure S5, except for 850 hPa except contour intervals for wind plots range from -5 to +5 ms^{-1}.

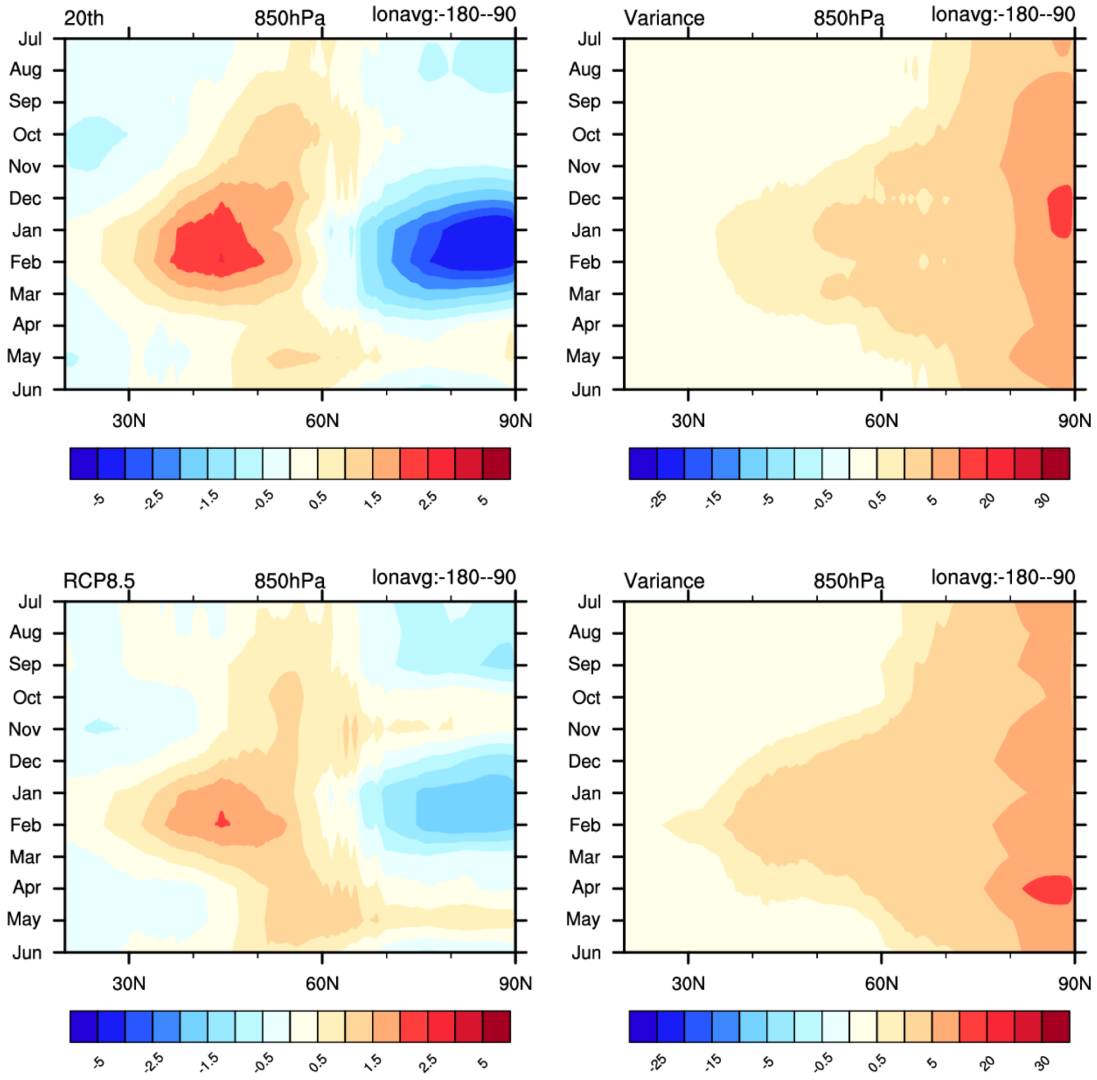

Figure S7. Same as Figure S5 (300 hPa) except for European domain (50W-30E).

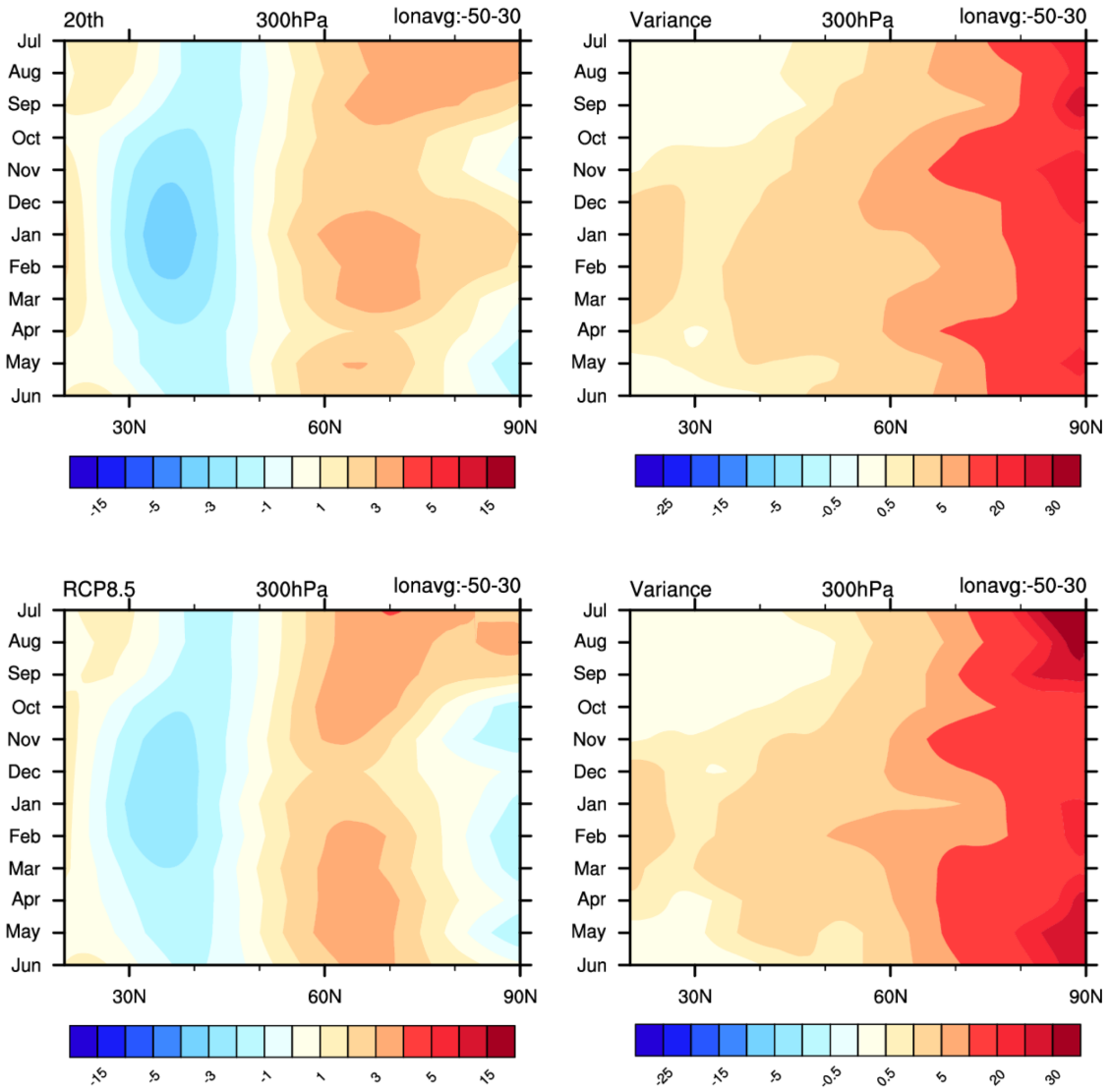

Figure S8. Same as Figure S7 except for 850 hPa.

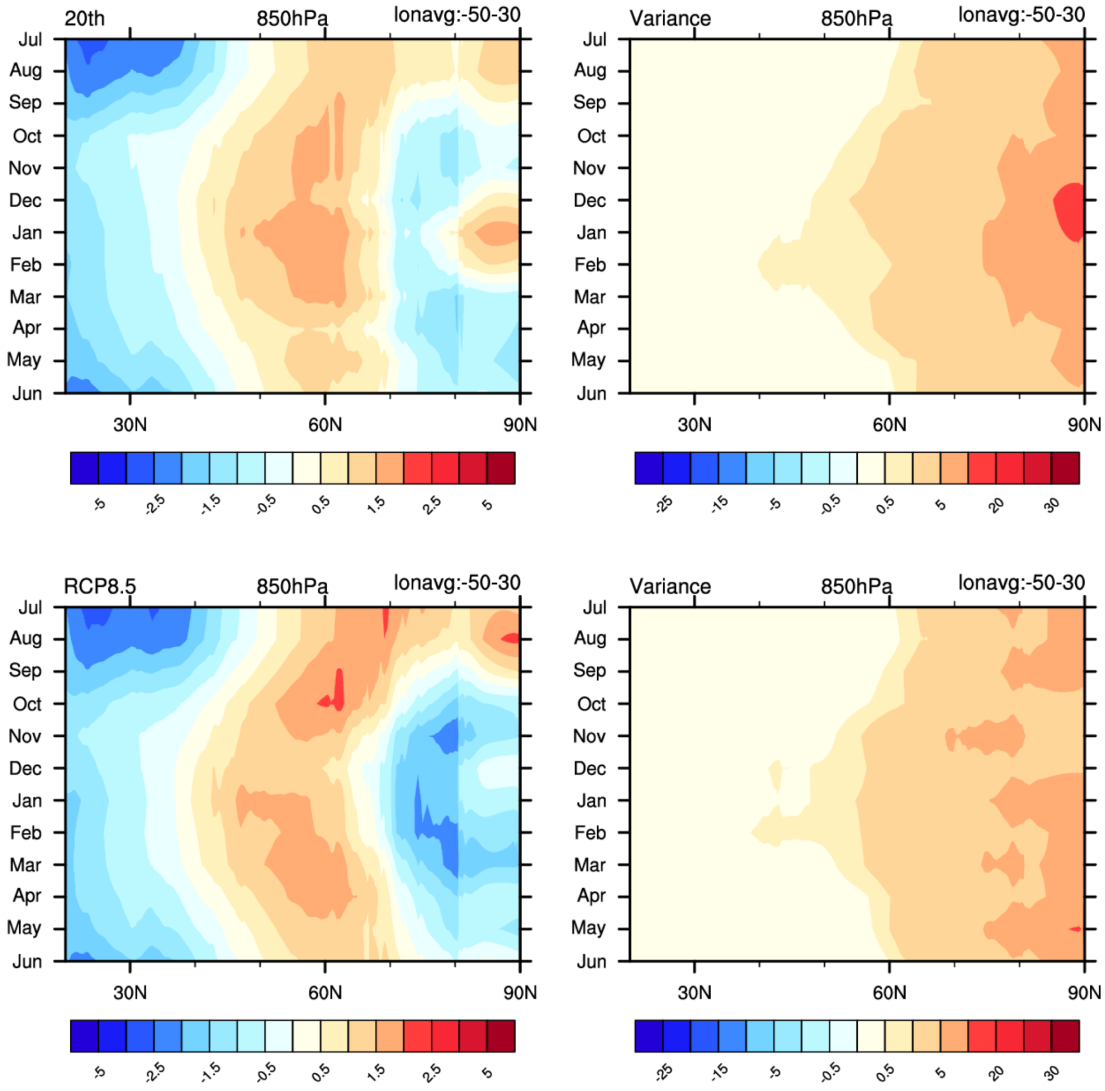

Figure S9. Western North American climate change (RCP8.5 – historical) mean annual cycle for 300hPa and 850hPa air temperature (^{o}C, upper left and right panels, respectively), and specific humidity (g/kg, lower left and right panels, respectively) for the life cycle domain (180-90W). The coastline domain (110-130W, not shown) signals are very similar in pattern and magnitude. All differences are significant to the 95% level and data is computed from monthly mean data, years 2070-299 (RCP8.5) and 1960-2005 (Historical). This plot is a companion plot to Figure 4.

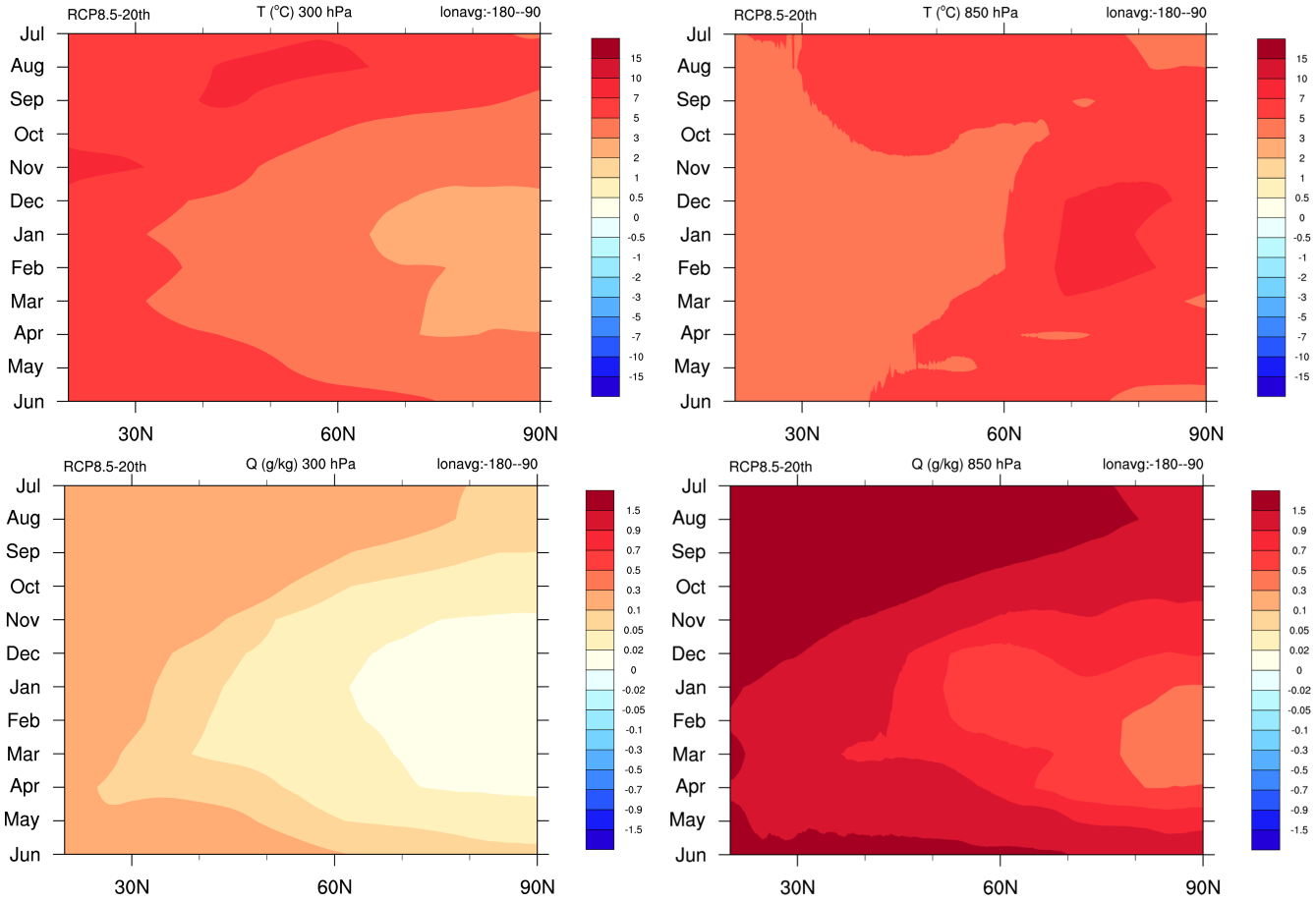

Figure S10. Same as Figures S9 except for the European domain (50W-30E). The coastline domain (30W-0E, not shown) signals are very similar in pattern and magnitude. This plot is a companion plot to Figure 5.

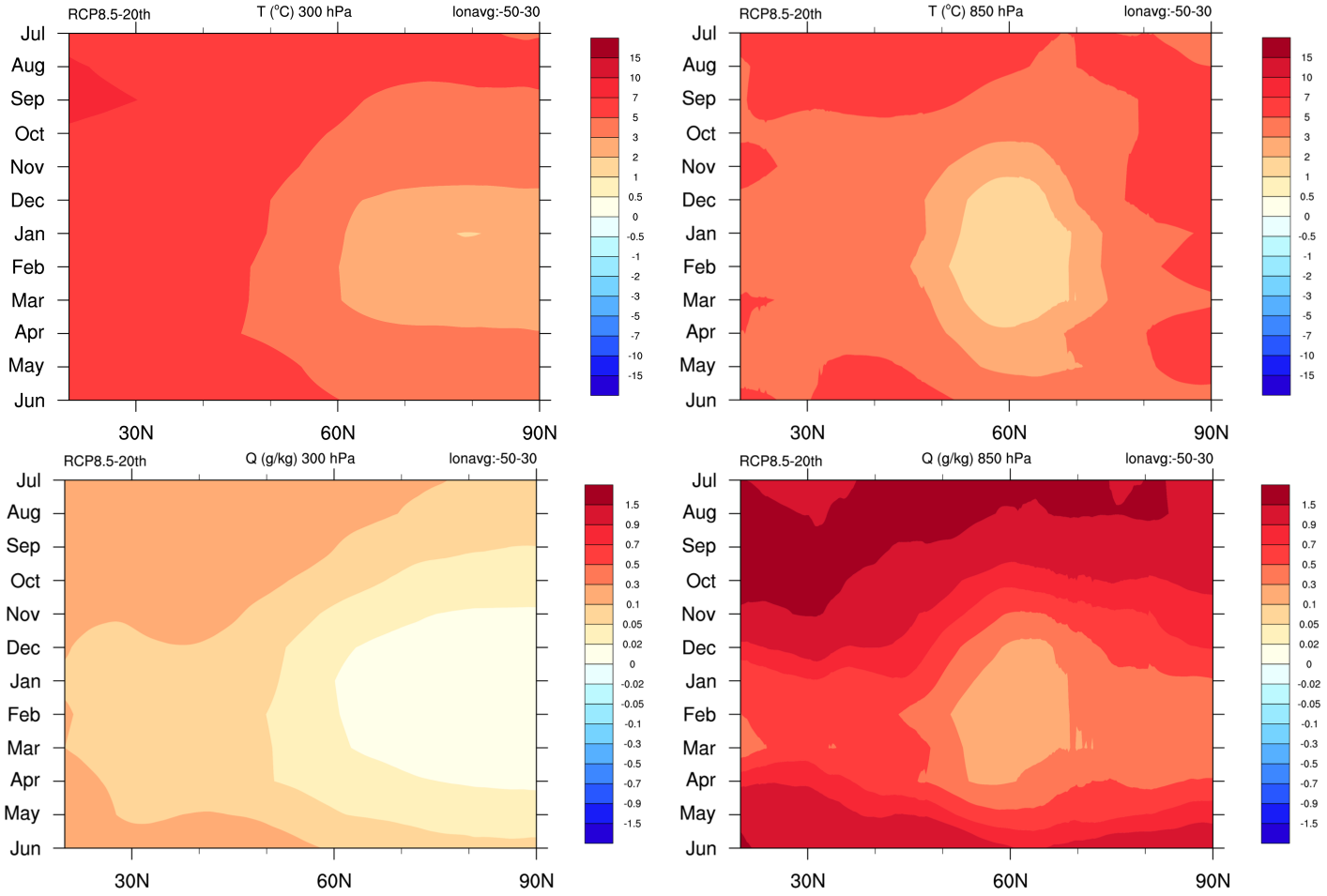

Table S1. Summary of ARTMIP Tier 1 catalogues applied to MERRA-2 reanalysis data for heat transport calculations. For more details, see ARTMIP algorithm webpage, http://www.cgd.ucar.edu/projects/artmip/algorithms.html). Full citations are found in the reference section of the main paper.

Developer	Regional Coverage	DOI Reference
Brands (v1, v2, and v3)	WNAM, UK, Ib	10.1007/s00382-016-3095-6
CASCADE (IVT and IWV versions)	Global	Mahesh and O'Brien (Experimental)
CONNECT (IVT 500 and 700 $kgm^{-1}s^{-2}$ versions)	Global	10.1002/2013EO320001 10.1175/JHM-D-14-0101.1
Gershunov et al. 2017, v1	WNAM	10.1002/2017GL074175
Goldenson, v1-1	WNAM	10.1175/JCLI-D-18-0268.1
Guan and Waliser	Global	10.1002/2015JD024257 10.1175/JHM-D-17-0114.1
IDL, v2s	UK, Ib	10.5194/esd-7-371-2016
Lavers	UK	10.1029/2012JD018027
Lora (Global v1 and Lora v2)	Global	10.1002/2016GL071541
Mundhenk v2	Global	10.1175/JCLI-D-15-0655.1
Payne and Magnusdottir	WNAM	10.1002/2015JD023586 10.1002/2016JD025549
PNNL v1 and v2 (Hagos et al. and Leung_Qian)	WNAM	10.1175/JCLI-D-14-00567.1 10.1029/2008GL036445
Rutz	Global	10.1175/MWR-D-13-00168.1
Shields and Kiehl, v1	WNAM, UK, Ib	10.1002/2016GL069476 10.1002/2016GL070470
Muszynski et al. (Machine learning)	Global	10.5194/gmd-2018-53
Tempest (250, 500, and 700 $kgm^{-1}s^{-2}$ versions)	Global	Experimental
Walton, v1	WNAM	Experimental

Table S2. Summary for data used in analysis including period, simulation, and application. *Heat transport terms were limited by available data. For consistency, the climatology for the meridional wind was computed using the ensemble member where the heat transport data is available.

	Historical (# ens members)	RCP8.5 (#ens members)	MERRA-2
AR Tracking	1960-2005 (3)	2070-2099 (2)	1980-2016
Heat Transport Terms	1991-2005 (1) *	2070-2099 (1) *	1980-2016
Meridional Wind Climatology	1960-2005(1) *	2070-2099(1) *	1980-2016